SPE 8846

SPE
Society of Petroleum Engineers of AIME

ROCK STRUCTURE AND TRANSPORT THEREIN: UNIFYING WITH VORONI MODELS AND PERCOLATION CONCEPTS

by Prabodh Pathak, Phillip H. Winterfeld, H. Ted Davis, and L.E. Scriven, University of Minnesota

This paper was presented at the First Joint SPE/DOE Symposium on Enhanced Oil Recovery at Tulsa, Oklahoma, April 20-23, 1980. The material is subject to correction by the author. Permission to copy is restricted to an abstract of not more than 300 words. Write: 6200 N. Central Expwy., Dallas, Texas 75206.

ABSTRACT

Matrix and pores of rock form irregular, interpenetrating, network-like structures with interrelated shapes and connectivities that are statistical variables resulting from the nature of the original sediments and the diagenetic processes they have suffered. Transport properties of either network depend on geometry, i.e. size and shape distributions; transport depends equally on the number of transport paths, or distribution of connectivity, i.e. topology. Thus different structural properties and transport processes in rock matrix and in pore space are interrelated.

This theoretical prediction is studied by means of the Voronoi construction for subdividing space, which provides precisely defined, realistically irregular models of rock and of distributions therein of fluids, conductivity, permeability, strength, etc. Geometry and topology of the models are coded into matrices that are useful for thinking about structure and transport, and which become factors in illustrative calculations of electrical conductivity, Young's modulus, and fracture strength as functions of, for example, porosity. The results show percolation thresholds: cessation (or onset) of transport when a critical fraction of paths is randomly blocked (or created). Statistical features of structure and transport are the subject of percolation theory.

The results help focus experimental studies and point to a unified picture of structure, strength, and transport.

INTRODUCTION

Reservoir rocks are porous materials that because of their origins and history are partially ordered yet irredeemably chaotic. Their profound *irregularity* has defied adequate analysis and hindered understanding. Obviously some statistical concepts are needed, but distribution functions of pore sizes and grain sizes have not led deep. The reason is that the *geometry* of pores and grains is only half the structure of a rock. The other half is the way the pores are connected together — in a word, the *topology* of the rock structure. The connection patterns of the pores and of the matrix, however chaotic both may be, are not independent. Does this mean that mechanical properties of the solid matrix are related to fluid distribution properties and fluid flow properties of the pore space, and vice versa? Are there scientific bases for systematically incorporating all the conveniently measurable properties of rock in a geologically sound, physically accurate description useful for engineering the improved locating and recovering of oil?

A unified picture of rock structure and transport therein is indeed emerging, as we indicate here. At the center of this picture are new means for modelling the statistical geometry and statistical topology of rock, and new concepts for dealing with essential aspects of the innate irregularity.

Reservoir rocks are the "packed beds" in which oil becomes entrapped as residual, and in which chemical flooding processes are operated to enhance oil recovery. In trying to understand the distribution and flow of oil and brine in reservoir rock we discovered[1,2] that concepts and results of a comparatively new physical theory fit porous media beautifully: the *percolation theory* of transport through irregular networks and in irregular composites.[3-6] Most of the mathematical development of the theory is for circumstances in which the irregularity has major elements of randomness, but the theory is not restricted to entirely random structures. We perceive that it can be amended and extended to explain and correlate most of the peculiarities of deformation, strength, and transport in rock.

Many field observations and laboratory results can be explained qualitatively with percolation concepts. In its present state of development, however, percolation theory yields quantitative predictions in few cases except by Monte Carlo calculations with a model of the porous medium. It is also true that even the most careful laboratory experiments are confounded by the enormous time and expense of disassembling just a small sample of rock grain-by-grain, pore-by-pore, and recording all of the relevant dimensions and connections.[7] For both theory and experiment what are

References and illustrations at end of paper.

needed are model rocks of precisely known statistical properties or — far better yet — of exactly known constitution and structure, from which statistical properties can of course be calculated.

In trying to understand microemulsions, which may be chaotically bicontinuous, multiply connected structures as reservoir rocks are, our colleague S. Prager introduced the Voronoi division, or tesselation, of space randomly into convex polyhedra,[8,9] an idea that is not well known although it has been used in theoretical metallurgy and in liquid-state theory.[6] Recognizing that the degree of randomness can be controlled and that the polyhedra can be rounded if desired, we have automated the Voronoi-type of construction for the digital computer.[10,11] As described below, this enables us to generate rocks of exactly known pore and matrix structure with which to make totally controlled experiments by computer simulation. Of course a computer-generated tesselation is also a plan for building a tangible porous medium.

Voronoi tesselations of area into convex polygons are suitable for pilot studies because the two-dimensional constructions are simpler and less expensive than three-dimensional ones. We summarize here the results of pilot studies of conductive transport,[10-13] including pore-wall and grain-boundary conduction,[11] elastic deformation,[14] and microcracking and fracture.[14] Similar studies of fluid entrapment[15] and other processes are in progress. The results testify to the relevance of percolation theory and point to the unified picture mentioned above. They shed light on the extent to which regular lattices and networks, which are sometimes used as models, reflect the nature of porous rock. The results also help focus related laboratory experimentation with rock and kindred porous media at Minnesota and elsewhere.[7,15-17]

MODELLING ROCK STRUCTURE

Depending on the nature of the original sediments, the environment in which they collected, and the diagenetic processes they subsequently suffered, the pore space of sedimentary rock is more or less chaotic, and so is the solid matrix. In the chaos may be elements of order, such as bedding planes, however. The history of a reservoir rock is cartooned in two dimensions in Fig. 1. (a) pictures a volume of space just above the sea bottom: it is devoid of sediment. In (b) sediment grains have settled to form a high water-content deposit in that same volume. Close inspection reveals layering, the bottom layer containing the largest grains on the average. As this deposit is buried the grains shown will rearrange by stress-induced rotation, sliding, plastic deformation and perhaps even some breakage. In (c) the compacted sediment is lithifying. The pore space is filled with water transporting dissolved minerals that participate in cementation, dissolution, recrystallization, etc.; at the same time the matrix is stressed in complicated ways that influence solution and crystallization and may cause sintering or microcracking. Or (c) might show developing secondary porosity after an episode of massive cementation.

In (d) the pore space has been invaded by migrating petroleum which has accumulated to a high enough saturation that it is connected and can readily flow under a pressure gradient. Before much of a pressure gradient appears the assembly will probably have responded to low frequency, low amplitude elastic waves and, if it happens to be grazed by a bore-hole, to applied electrical potentials and other means of probing. Incidentally, (d) does justice neither to the water layers adhering to many of the grain surfaces that face oil, nor to the water-filled perforated-sheet micropores between some of the otherwise cemented or sintered grains. In (e) the specimen has responded to one after another of the pressure gradients that are typically applied in primary and secondary production of a reservoir. The residual oil that remains has been disconnected by the conspiring of pore configuration and capillarity and it is held trapped by the same conspiracy. There are many reasons for seeking to model rock structure in such a way as to capture the essential features despite the camouflage of chaotic irregularity.

Several kinds of porous media appear to bracket rock. One is the familiar unconsolidated pack of well-rounded grains or beads all of nearly the same size; limiting forms are the geometrically and topologically perfectly regular sphere packs, in which the coordination number of the grains is fixed and so is that of the pore bodies. A second kind is the unconsolidated pack of nearly identical polyhedral grains; again there are perfectly regular limiting forms. Both kinds can be cemented or partly sintered and fused to resemble consolidated sedimentary rock more closely. However, it appears that all of these relatives as well as rocks themselves can be approximated as space-filling assemblages of polyhedra — polygons in two dimensions — some of which are grains, or solid matrix, and the others of which are pores, or fluid-filled space. The polyhedra — or polygons — should generally not be regular. Fig. 2(a) shows the board on which the game of Fig. 1 was played; in subsequent panels of Fig. 2 the game is replayed.

Voronoi Tesselation

To develop the rules of modelling rock by the method of polyhedra (as noted above, once a model is constructed the polyhedra in it can be rounded as appropriate) it is convenient to start with cases of exclusively convex polyhedra. A quite flexible and potent approach is provided by the Voronoi construction for subdividing space randomly or otherwise into convex polyhedra; the construction can be executed by computer. Fully random Voronoi tesselations of *area* into convex *polygons* of prescribed mean area are suitable for pilot studies because, as already noted, they are simpler and less expensive than three-dimensional construction. The examples in this paper are based on such tesselations, the construction of which is outlined in Fig. 3. Within the polygon about a Poisson point are all points lying closer to it than any other Poisson point. The Poisson points are merely scaffolding for the construction and can be removed afterward. But when the Poisson points are chosen entirely randomly there can be none of the stratification shown in Figs. 1 and 2. The random tesselations actually used in a number of the examples are shown in Figs. 4 and 16.

Representation by Matrices

To represent the structure of connections in a tesselation, i.e. which of the polygons (polyhedra) border each polygon (polyhedron), it is convenient to replace the tesselation by a network. The essence of the network can be stored in a table or array, but it is helpful to visualize it as in Fig. 4(a), where the centroids of the Voronoi polygons are the nodes and adjacent nodes are connected by branches, or bonds,

each of which corresponds to a common side of two polygons.

To represent the geometric shapes in a tesselation it suffices to tabulate the coordinates of polygon (polyhedron) vertices in a systematic way. However, for many computational purposes it is convenient to dissect each polygon (polyhedron) into triangles (tetrahedra). This is illustrated in Fig. 4(b), where the same tesselation has been broken down into triangles by drawing straight lines between the centroid and vertices within each polygon. All of the information about shape is contained in the lengths of the triangle sides, which for ready reference by computer methods can be recorded in an array, or matrix T, the rows corresponding to the triangles and the columns to the sides (other arrangements are useful for various purposes). A crude numerical index of shape is merely the ratio of the length of a polygon side to the distance between adjoining centroids or, alternatively but less defensibly, to the distance between adjoining Poisson points. Indeed, this index is used below to approximate the transport resistance between the two polygons when for simplicity the tesselation is fully replaced by a network of transport paths derived from it.

Converting a tesselation into a model of rock is a matter of deciding what fraction of the polygons (polyhedra) are matrix, what fraction are pore space, and what degree of order, if any, there is in the split. In the examples used here the split is entirely random. Now the matrix network and pore network are efficiently represented by an incidence array, or matrix, the rows of which are the polygons, or nodes, and the columns of which are the polygon sides, or branches. The entries are letters (or numbers, which are better suited for the strength and transport calculations summarized below) that denote the composition or filling of each polygon: see Fig. 5.

The entire connectivity structure, or topology, of the model rock and its pore filling is recorded in this rectangular incidence matrix C, relatively simple cases of which are standard fare in network science and engineering.[18] It is remarkable that according to matrix algebra, if C^T is the transpose of C, i.e. the matrix in which its rows and columns have been interchanged, then the i-th diagonal entry of CC^T, a square matrix, is the number of sides of the i-th polygon times the "square" of the symbol of its composition (WW, SS, or OO in Fig. 5); the off-diagonal entries tell what polygons share common sides. The total number of sides a polygon has is of course its coordination number in the tesselation. The number of sides it shares with polygons of like compositions is its coordination number in the network of that composition, and this number can be counted up in the off-diagonal entries in its row (or in its column, equally well). The coordination number of a pore polygon is the number of ways out of that part of the pore space into other parts, and thus characterizes the local topology of the pore space. The coordination number of a rock polygon has the same sort of significance, and can be counted up in the same fashion. All of the information is in C.

Polygons (polyhedra) unless they happen to be totally surrounded by another kind are part of a larger structure, the grains or pores of which can be identified systematically from C and shape information once definitions of grain boundaries and pore throats are adopted. The connectivity of the matrix and the connectivity of the pore space can be calculated from C, as can the local measures, the coordination numbers of grains in the network of solid and of pores in the network of pore space. (Indeed, C can be broken down into C_S for solid and C_P for pore space.) What is extremely significant is that the coordination numbers in two interpenetrating networks are interrelated and their connectivity properties are conjugate; that is, *the topology of the rock structure follows from that of the pore structure, and vice versa.*

When oil and water compete for pore space it is in effect divided into two spaces: see Fig. 5(c). Continuous fillings of oil and disconnected oil blobs or ganglia can be likewise be calculated from the incidence matrix C. Again it is extremely significant that the connectivity properties of the water-filled and oil-filled networks are conjugate; *given the topology of the pore structure, the topology of oil-filling follows from that of water-filling, and vice versa.*

Interestingly, the j-th diagonal entry of C^TC, a square matrix of higher dimension, is the "square" of the symbol of one polygon plus the same of a contiguous polygon (e.g. WW + WW, WW + SS, etc. in Fig. 5). That is to say, the diagonal entries of C^TC summarize the network of the original tesselation from the point of view of branches while the diagonal entries of CC^T do the same from the standpoint of nodes. The same is true of C_S and $C_S{}^T$ for the solid matrix, C_P and $C_P{}^T$ for the pore space, C_W and $C_W{}^T$ for water-filled pores, C_O and $C_O{}^T$ for oil-filled pores, and so on. In C resides all of the information about structure of a model rock, apart from local shape. In another matrix, either T, the matrix of side-lengths in a triangulation which was introduced above, or an equivalent array, resides all of the information about shape. It may be helpful to think of C as the skeleton and T as the flesh; if the analogy is pursued the property matrices in the next section are the tailored clothes that make the person.

MODELLING TRANSPORT

Change of, and within, a rock is brought about by transformation processes such as phase transitions and chemical reactions, and by transport processes such as electrical conduction, heat conduction, molecular diffusion, and fluid flow, and also by elastic deformation and plastic deformation, which can be viewed in terms of momentum transport. The modelling of change in rock models built on Voronoi tesselations as well as less random constructions is clear in outline, but details have been completely worked out so far in just a few pilot studies for the numerous modelling efforts under way at Minnesota. Some of these pilot studies are of transport, ostensibly Ohm's-law electrical conduction in pore space but simultaneously of Fourier-law heat conduction, Fick's-law solute diffusion, and Darcy-law flow of a single fluid, owing to the close analogies among these processes, as indicated by the familiar, simplified constitutive relations shown in Fig. 6. Hooke's law is taken up below.

Transport Properties

The constitutive relations in Fig. 6 are simplified ones for steady one-dimensional transport down a path along which the transport coefficient is constant. The simplification is appropriate when a polygonal (polyhedral) model is replaced by a network in the manner described above. The question then is how to assign conductances or permeabilities to the branches of the network in order to approximate well the

transport process in the model. The conductance of a transport path obviously depends on the conductivity of the material of which the path is composed *and* on the shape of the material, e.g. its cross-sectional area as a function of distance along the path. If the material is inhomogeneous — as is generally the case in rock — the conductivity is distributed. But the shapes in an irregular polyhedral model always are distributed, and consequently in pilot studies it is appropriate to begin by supposing the material properties are homogeneous and the branch conductances are controlled by geometric shape. An intuitively attractive approximation introduced by Hatfield[10] is to set the conductance of each branch proportional to the length of the side between polygons that it represents, and inversely proportional to the distance between centroids or, more simply, the Poisson points of the two polygons, as indicated in Fig. 7. That this is a reasonable approximation is established by the more accurate calculations for polygonal models which are outlined below.

Representation by Matrices

The conductances in a network approximation to a polygonal (polyhedral) model are efficiently recorded as the ordered diagonal entries in a purely diagonal matrix K having as many rows as there are branches, or bonds, and an equal number of columns (thus the dimension K is that of CC^T); the off-diagonal entries are all zero. For some purposes the branch resistances, which are merely the reciprocals of the branch conductances, are needed; these are efficiently recorded as the diagonal entries in a purely diagonal matrix R of the same ordering and size. So far as the transport process is concerned, the matrix K or R supersedes the shape information in T, which was introduced above. Indeed, when conductivity is uniform K and R can be calculated from nothing more than T and the value of the conductivity. What is highly significant is that the conductances and permeabilities for different transport processes in the same network of paths — rock matrix, pore space, water-filled pores, oil-filled pores — are necessarily related because they depend on shape along paths in similar though not necessarily identical fashions. Darcy-law permeability, for example, is more sensitive to cross-sectional constrictions than is Ohm's-law conductance. Nevertheless, *the geometric shape of rock matrix closely links the transport properties in different transport processes in the matrix; the geometric shape of pore space likewise closely links properties in different transport processes in the pore space; and the interrelation of matrix shape and pore shape links, to some extent at least, transport processes of the two kinds.*

The geometric shapes of oil-filling and water-filling affect transport processes within the pore space in similar ways as do the pore shapes themselves. Thus geometry is half the structure of a rock and of its pore fillings, while topology is the other half. This can be seen vividly in the matrix formulation of electrical conduction or an equivalent process in, say, the pore space of a polygonal rock model generated by means of a Voronoi tesselation. Two such formulations appear in Fig. 8.

Transport Formulated Mathematically

When current or flux is impressed at the boundaries of the specimen, it may be simpler to solve first for the potentials ϕ_i at the nodes of the network and then calculate the fluxes throughout; this is the strategy behind the potential formulation in Fig. 8(a). When potentials are impressed, it may be simpler to use the flux formulation in Fig. 8(b) and solve first for the currents I_j. (In the flux formulation the connectivity structure is represented by a current-loop incidence matrix D which is derived from C and appears instead of C.[18]) Actually the numerical work is often less by that formulation which presents fewer simultaneous equations to solve. It turns out that the number of independent equations in the flux formulation is less than in the potential formulation when the network is not too holey, i.e. when there are not many closed loops in the network. In any but the smallest specimens of porous rocks having appreciable permeability the holeyness of the transport networks in both the matrix and the pore space is immense and begs for statistical treatment once its essential aspects are understood from the studies of model rocks which are in progress.

What is striking about both formulations is the way that topological structure C (here with 0 and 1 replacing S and W and a sign convention introduced) or D multiplies geometric-shape-determined conductance K or, respectively, resistance R to produce the coefficients of the unknown potentials or fluxes in the sets of linear, algebraic equations. In matrix notation the arrays in Fig. 8 boil down to

$$(CKC^T)\phi = I_b + CK\phi_b$$

$$(DRD^T)I = \phi_b + RI_b$$

Here is a powerful means for thinking about rock structure and transport therein, even though modern computers can still not solve enough equations to analyze in detail anything more than a pathetically small specimen, from the viewpoint of reservoir engineering. Again, what is needed is a statistical treatment that adequately relates the essential aspects at smaller scales to the important aspects at larger scales.

RESULTS OF TRANSPORT MODELLING

Sample solutions of the equations in Fig. 8 have been obtained by Hatfield[10] and Winterfeld[11-13] for conduction in two-dimensional networks, some regular, some Voronoi-generated, in which the branches are randomly chosen to be conducting in various proportions. Selected results for a tesselation containing 160 polygons are graphed in Fig. 9(a). What is noteworthy is that the specimens on the average conduct not at all until over 40% of the potential paths between polygons are conducting. This type of threshold behavior is well-known in chaotic networks and chaotic composites: it is called a percolation threshold, it is a subject of percolation theory, and it is taken up below. In that regard the cluster-distribution results shown in Fig. 9(b) are of interest.

Finite Element Analysis of Conduction

Conduction in polygonal models, including those behind the network model in Fig. 9, can be analyzed more accurately — indeed, as accurately as expense and computer limitations allow — by the methods of subdomains and Galerkin weighted residuals in the modern combination known as finite element analysis.[19] That is, novel developments in computer-aided analysis now make it possible to approximate as closely as desired the solutions of Laplace's equation and other partial differential equations of transport when the

domain is chaotic or random as are those generated by Voronoi tesselation. In the case of Laplace's equation in two dimensions it happens that the potential formulation leads to a useful upper bound on the reduced conductivity while the flux formulation leads to a useful lower bound; the reduced conductivity is the conductance k of the polygonal model divided by the conductance k_0 when the entire tesselation is filled with conducting material.[12,13]

The results labeled "coarse" in Fig. 10 are for a 160-polygon Voronoi tesselation (shown in Fig. 16(a)) in which each proportion of conducting polygons was realized by random choices 10 times. The conduction problems were solved with finite element bases consisting of linear trial functions, called chapeau functions, on elements that are the triangles into which the polygons can be dissected as in Fig. 4(b); the mean and standard deviation of the ten reduced conductivities in each set are indicated in Fig. 10. There the results labeled "refined" are from more accurate finite element calculations in which each triangle was systematically subdivided into four in the usual way.[19] The rates of convergence of the upper and lower bounds are about the same and the true reduced conductivity can be estimated with an error likely to be less than 1%, which illustrates the potency of the method.[12,13] Here, then, is an example of model rocks of exactly known constitution and structure from which statistical properties — matrix conductivity or pore conductivity in this case — can be accurately calculated. Incidently, the results show that a resistor network tends to have a bit lower conductivity than the polygonal model from which it is derived. The percolation threshold is again evident, at a conducting fraction of about 45%.

Pore Wall and Grain Boundary Effects

Pore-lining clay minerals and imperfectly cemented grain boundaries or perforated-sheet-like micropores if filled with brine apparently can affect strongly the conductivity of reservoir rock. These phenomena are roughly accounted for by Archie's "law" and similar correlations. They can easily be investigated with suitably designed modifications of the model rocks used for Fig. 10.[11] In one modification the pore surfaces are assigned a special conductivity k; the results are shown in Fig. 11(a). The percolation threshold is unaffected but if the surface conductivity is sufficiently high the surface conductance overshadows conduction through such conducting liquid as is present in the pore space. In another modification not only the pore surfaces but also the grain boundaries are assigned the special conductivity k, with the results shown in Fig. 11(b). Now there is no well-defined percolation threshold because even when all of the polygons are nonconducting — whether they are solid rock or oil-filled pore space — the surface and grain boundary paths remain, although their conductance may be low.

Network Analysis of Young's Modulus

To this point the transport processes that have been modeled are described by linear equations. Whereas Hooke's law of elasticity in one dimension is linear, it is not in two and three dimensions except at vanishing strains (see Fig. 6). Young's modulus at vanishing strain of dry rock is an interesting example. Properties related to or similar to this momentum-transfer modulus are of course of great importance in locating and assessing reservoir rock. Elastic deformation of consolidated rock is more complicated than conduction because the rock resists both bending strain and tensile or compressive strain. To be realistic a network model accordingly ought to consist of trusses that can be bent as well as stretched or compressed; moreover it seems reasonable to take the trusses as being rigidly bonded to each other. Fig. 12 portrays the relation between force components, F_x and F_y and bending moment M_z at a network joint or node, and the displacements Δx and Δy and rotation $\Delta\phi$ of the joint.[20] The elastic properties depend on Young's modulus E of the matrix material and the local shape, as represented by cross-sectional area A, length L, and moment of inertia I. The relations in Fig. 12 can be assembled into matrix equations for elastic deformation of a Voronoi-generated, two-dimensional network in which the branches are randomly chosen to be trusses or void in various proportions.

Results for a tesselation containing 200 polygons are plotted in Fig. 13, where porosity stands for the proportion of network branches that are void. Shown are the mean and spread of five random realizations at each porosity.[14] Also shown are the mean and standard deviation of more than 50 sets of measurements of Young's modulus of ceramics and glasses.[21] The novel truss-network model reproduces, to within a constant factor, the oft-measured behavior of ceramics. The constant factor, we believe, comes from the difference between the two-dimensionality of the pilot models and the three-dimensionality of the measured specimens; in random structures of the same porosity, scale and local modulus, there are more interconnections in three dimensions and hence the three-dimensional structure ought to be stiffer.[14]

Microcracking and Fracture

If the tensile strengths of bonds between adjacent polygons in the underlying model are specified — and they can be realistically distributed, if desired — the analysis can be extended to bond failure and beyond, i.e. to truss failure in the network, which corresponds to microcracking in the rock model. With each microcrack a load-bearing branch of the network disappears and so the topology changes; hence the incidence matrix C must be altered with each successive microcrack and a new elasticity problem solved. (The situation is similar in two-phase flow when as oil saturation falls, capillarity conspires with pore geometry to force breaks in the oil continuity, as sketched below.) Each solution, incidentally, yields a Young's modulus of rock under successively greater strain. The results show how, as uniaxial compressive strain is increased, tensile microcracks form and multiply until a maximum supportable stress is reached: see the example in Figs. 14 and 15. When this stress is exceeded the already present clusters of microcracks rapidly link up and fracture ensues. This is another example of a percolation threshold. The modelling can be further extended to account as well for the shear strengths of bonds. The maximum supportable stress is the gross strength of the model rock. Its variation with porosity reproduces, also to within a constant factor, the general trend of the many measurements of strengths of ceramics.[14,21]

These findings indicate that mechanical properties, including strength, of rock can be modeled by means of the Voronoi construction — adequately by the network approximation, and still more accurately by finite element analysis of elastic deformation of the polygons (polyhedra), which is in the offing though it is more

demanding than the finite element analysis of conduction sketched above. No other conceptual framework in the literature accounts for the observed porosity dependence of all four aspects of compressive loading of ceramics and rocks: (i) elastic moduli at small strains; (ii) numbers, length and orientation distributions of microcracks as strain increases; (iii) inelastic stress-strain, fracture strength, and post-critical stress-strain; (iv) sensitivity to anisotropy of loading, which can convert brittle fracture to ductile fracture, as indeed the Voronoi-generated truss-network models show.[14]

FLUID DISTRIBUTIONS AND FLOW

Flow of a single fluid phase through pore space is described macroscopically by Darcy's law and variants. Microscopically it is being modelled by the methods already described, for such purposes as understanding Darcy's law and flow distribution, wall shear that tends to tear off fines, adsorption rates at pore walls, effects of graded viscosity, and various dispersion mechanisms. When two or more immiscible phases share the pore space, what is central is how they are distributed — first of all when they are not flowing. The case receiving the most attention is that in which the reservoir rock is totally wet by water or brine and an immiscible oil phase is also present. In this circumstance the walls of otherwise oil-filled pores are, by definition, lined by thin films of water. The evidence is that the static distribution of oil and water is controlled by pore configuration, with capillarity — the action of interfacial tension between oil and water at curved menisci — being its agent. The distribution is also influenced by the history of past flow.

Pore Shape and Fluid Distributions

Pore walls are necessarily curved; even when they are faceted as in polyhedral porous media there are singular concentrations of curvature in the seemingly sharp corners and edges.[22] It happens that *the distribution of wall curvature is related, according to topological facts, to the connectivity of the pore space or, equivalently, to the connectivity of the rock matrix.*[22,23] Necessarily there are wall regions having reverse curvature (principal curvatures of opposite sign) and hence local saddle shape: these regions must include the pore throats and the matrix necks. *Thus pore shapes, and matrix shapes as well, are linked to the interrelated topologies of the pore structure and the rock structure.* The pore throats are not only cross-sectional constrictions, they are also the wall regions of lowest mean curvature. As a consequence they exert controlling influence on the distribution of oil as its proportion, or saturation, falls and capillarity is present in water-wet rock.

At high oil saturation most of the pore throats are filled with necks of oil although the throat-walls are coated by water in a thin-film state.[24] The oil in the pore space is continuous, i.e. well connected. As saturation falls, collars of bulk water tend to grow around the necks in the throats and then to suffer a capillary instability that causes them to choke-off the necks, first of all those in the most constricted throats and then, as oil saturation continues to fall, in larger and larger throats. When the instability chokes off a neck it breaks an oil connection and creates two menisci called heads, i.e. concave oil-water interfaces, that retract toward stable locations in nearby pore bodies. As they do so they may sweep past adjacent connecting throats and sever the necks in them so that additional heads are formed. (The process is analogous to microcracking of the matrix under load, and can be analyzed by the methods described in the preceding section.) The heads that are created take up stable positions, many of them next to the larger pore throats; but as saturation falls they too may suffer another capillary instability and jump — Haines' jump — through larger pore throats to new positions, severing necks and creating new heads as they go.[25]

In these ways more of the menisci called heads are generated as oil saturation falls, and always the cause is *instability* of an interface configuration that is controlled by the distribution of pore-wall curvature. The succession of meniscus states is completely determined, given the initial state, if interfacial tension is appreciable and viscosity low enough that the viscous effects accompanying motion are insignificant. This is roughly the picture in primary production, for example, although the presence of gas is generally a complicating factor. In waterflooding and chemical flooding there is usually a migrating oil bank the rear of which is a moving zone of falling saturation in which oil connectivity is repeatedly broken by the events that populate the zone with heads; these events are essentially those just described if the Darcy-flow velocities are low enough that capillarity dominates viscous effects, i.e. at normal waterflooding capillary numbers. (A static oil-water or gas-oil contact region in reservoir rock is a similar falling-saturation zone at rest.) With increasing numbers of breaks in oil-phase continuity, portions of oil become totally disconnected from the continuous oil. These portions, which may occupy from one to many, many interconnecting pore bodies, are called blobs or ganglia (they may also be regarded as clusters); each is surrounded by the menisci called heads and by water-wetted rock surface. The number of breaks required on the average to create a blob depends on the connectivity of the pore space; in particular, it depends on the average coordination number of a pore — the number of ways out.[26]

The disconnected blobs, if they are shorter than a calculable length that depends on the pore space and the capillary number of flow (or the Bond number of gravitationally-caused buoyancy), cannot move: they are trapped, again by a conspiracy of capillarity and pore configuration.[16] Disconnected and trapped, these blobs are lost to the network of paths over which oil previously flowed, unless they are rescued by arrival of, and coalescence with, some blob long enough to be in motion. Given the rock structure, and, in flooding, the overall flow direction, the entire sequence of events is in principle deterministic and reproducible. At any saturation value as saturation falls from a given initial value, the number and location of choked-off necks is fixed. So are the number and location of isolated blobs as well as of still continuous oil. In other words, the cluster-distribution when viscous effects are insignificant depends on the configuration of the pore space and saturation only (apart from hysteresis effects, i.e. influence of the initial distribution and reversal of saturation change). When saturation falls to a certain level set primarily by the connectivity of the pore space, the last remaining continuous paths of oil through the rock are, on the average, broken: a percolation threshold.[1,2]

At a slightly lower saturation value the additional instabilities and breaks in continuity of the longer, isolated yet movable or moving blobs leaves an entire population of trapped blobs, which are known collectively as the waterflood residual, i.e. the oil saturation that cannot be reduced further by brine flowing at any low capillary number. The experimental evidence, direct and indirect, is considerable.[2,26] And so it appears that *fluid distributions in pore space are results of transport processes that depend on the same geometrical and topological aspects of the rock as do other transport processes.*

Blob Mobilization and Capillary Number

Disconnected and trapped, a blob remains immobile even though aqueous phase continues to flow through nearby pores, as noted above, up to a critical value of capillary number — the ratio of dynamic viscous forces in the water that tend to move oil, to the capillary forces holding it trapped. The critical value hinges on the length of the blob in the flow direction and the pore dimensions in which it is trapped. The capillary hydrodynamics of blob mobilization and confirming experiments show that at the critical value one of the blob's head menisci becomes unstable in the throat where it is lodged and jumps ahead; often this mobilizes the blob.[15,16,22,26] If each such instability unfailingly and permanently mobilized the content of a blob, and if the blob-size or cluster distribution of residual oil were known at a given value of capillary number, then from blob mobilization theory could be predicted the incremental reduction in residual saturation upon incrementally increasing the capillary number with which the aqueous phase flows. In this way the entire curve of residual saturation versus capillary number starting from a given state of saturation could be constructed. Though blob-size distribution data are exceedingly rare, this has been done: the key is an application of percolation theory to the problem of a cluster distribution.[1,26] The entire process of entrapment and mobilization can be simulated in Voronoi models.[15]

Laboratory tests with water-wet systems have established that residual oil saturation following flooding with water or aqueous solution does indeed correlate with capillary number (aqueous phase Darcy flow velocity times its viscosity divided by its interfacial tension with the oil). At capillary numbers less than about 10^{-6}, which is the normal range in the field except around well-bores, residual saturation reaches a reproducible limiting value that varies primarily with the nature of the rock (cf.[26]). The differences in the limiting value are interpreted as differences in percolation thresholds owing to different average coordination numbers in various types and specimens of rock, or rock stand-in. As flooding rate or viscosity is increased or as interfacial tension is reduced by orders of magnitude, residual saturation falls gradually and begins to approach zero when capillary number climbs past 10^{-2}, which is evidently the range in which even the shortest of trapped blobs are mobilized unless they happen to be caged by pore throats that are together cross-wise to the adjacent flow. What is especially significant is this: if residual saturations at different capillary numbers are divided by the limiting residual saturation in the same specimen, then the curves of this ratio versus logarithm of capillary number are superposable merely by shifting the capillary number scale, for most of the specimens reported on in the literature.[26] This suggests that there is a universal feature of the residual saturations of oil in flooded regions that is independent, or nearly so, of the details of rock and pore structure. The feature should be sought in the distribution of residual saturation — the blob or cluster distribution — and the means for doing so is percolation theory, as touched on below.

The indication of a universal feature of residual saturations is significant in many respects, among them the common features in curves of capillary pressure (including initial/residual hysteresis) versus oil saturation, relative permeability variation with saturation and capillary number, results of tracer flow experiments, and others.[2,26] As important to understand as the common denominators are the differences that overlie them. Percolation concepts are appropriate tools. The degree to which they work in this area of fluid distributions and flow testifies to their more general applicability to structure and transport in rock.

PERCOLATION CONCEPTS

The term, *percolation*, was applied by Broadbent and Hammersley[3] to the process of generating a continuous transport path across a network or composite in which individual, short transport branches are created or activated more or less at random in increasing numbers. This is illustrated in Fig. 16. If there are very few active branches each of them is *isolated*. As the proportion rises, clusters of connected branches form (compare Fig. 9(b)); within the growing clusters the numbers of transport loops grow too. At any stage some of the clusters reach to one of the boundaries of the system; branches in these clusters are said to be *accessible*. When the proportion of present and active branches reaches a critical level, the probability of having at least one continuous transport path across an indefinitely large system becomes a virtual certainty. This proportion, the minimum fraction of network branches that must be active in order for a continuous transport path to be guaranteed, has come to be called the *percolation threshold*. Once the threshold is crossed, branches from which there are distinct paths to both boundaries lie on transport routes and are said to be *effective*; otherwise though accessible they lie on dead-end trails and are called *ineffective*. Typically the effective fraction rises rapidly just beyond the threshold as large, previously ineffective clusters get connected in.

Percolation theory deals with probability distributions of isolated, accessible, ineffective and effective parts of chaotic structures; with the statistical geometry and statistical topology of clusters; and above all with percolation thresholds. Thus it is the theory of connectivity and transport in irregular arrays of connections or transport paths, whether the underlying structure is as regular as a perfect crystal or as random as a Voronoi tesselation. Like diffusion theory it is statistical. Whereas conventional diffusion theory treats transport by random movement in a structureless medium, percolation theory treats transport by deterministic movement in a random structure or randomly structured medium. It establishes, for one thing, that the connectivity, and hence the number of transport paths, in a network depends on its "branchiness," as measured by the average coordination number of the nodes. The more connections each node has on the average, the greater the probability that branches meeting at it are effective in transport. Thus percolation theory finds application to such diverse processes as small atoms diffusing among the

chaotically ordered large ones in an amorphous solid, the spread of blight in an orchard — and, as noted above, to conductive transport in rock and Voronoi models thereof, to microcracking and fracture of porous media, to fluid distributions and to fluid flow in the pore space of rock. The theory is still young and far from fully developed, especially in mathematical rigor because, as we have seen, to make quantitative predictions most often requires Monte Carlo experimentation, albeit by computer.[4] A major challenge is to devise more effective ways of dealing theoretically with the partial ordering caricatured in Fig. 1 and so prevalent, in rocks for example. Such ordering tends to complicate statistical theory greatly. Nevertheless, the concepts and methods of percolation theory plainly apply to relating the statistical geometry and statistical topology at smaller scales in rock to important larger-scale aspects of structure and transport.

Cluster and Blob Distributions

A striking, encouraging case of the efficacy of percolation concepts followed on Larson's discovery that the cluster size distributions at *the percolation threshold* of a considerable variety of topologically regular structures are quite similar. These structures include many regular lattices and trees (a tree has branching without reconnection, a lattice has both) in two and three dimensions. In each the coordination number is uniform and thus the connectivity is regular, but the coordination numbers vary from 3 to 13. In these structures the percolation threshold varies inversely with coordination number, from a fraction of branches active in transport of 0.697 down to 0.083. That the populations of clusters at these widely differing thresholds are so alike, particularly in the smaller clusters that account for the bulk of the active branches remaining, appears to be due to the similarity of all of the lattices and trees after they have been pruned down to their respective percolation thresholds. Because the structures are pruned at random, their topological structures are quite irregular. It is reasonable to hypothesize that they are not much different from what is left of originally irregular structures, such as the continuous oil in relatively highly saturated rock, after they too are pruned down to their respective percolation thresholds, as by waterflooding.

This hypothesis offered an explanation for the apparently universal feature of the residual oil saturations after waterflooding, which is described above: the configuration of the disconnected oil, i.e. the blob distribution, does not vary greatly in its essential features from one porous medium to another. Inasmuch as all blob motion should cease at a saturation only slightly lower than the percolation threshold of oil continuity in a rock, this led to the decision to evaluate, by Monte Carlo calculation, the cluster size distribution of a 30x30x30 simple cubic lattice (extended by periodic boundary conditions) slightly below its percolation threshold of 0.320. From the same calculation the cluster *length* distribution in one direction was found and used as a model for the blob length distribution at waterflood residual, which was needed to predict residual saturation versus capillary number in the way sketched in the preceding section. The calculated cluster size distribution (and an earlier one evaluated from a Bethe tree[1]) agrees well with the one set of blob size data currently available.[26]

The outcome is a model that correlates the measured curves of the ratio of residual saturation to that at waterflood residual, versus capillary number -- with one parameter. The parameter relates to the critical mobilization length of blobs, depends on average pore shape characteristics of the rock, and simply shifts the capillary number scale underneath the universal curve. The correlation of residual saturation with capillary number is completed with a second parameter, the limiting waterflood residual (the residual at vanishing capillary number), which in the light of percolation theory and blob mobilization mechanics is virtually the percolation threshold of oil continuity and should therefore be closely related to the connectivity, or average coordination number, of the pore space.[26] More direct experimental confirmation is being sought.[7]

One of the issues reinforced by this practical outcome of percolation concepts is the character of the similarities and differences between structure and transport in two kinds of systems.[7,10,11] On the one hand are those like rock and Voronoi models, the underlying topology and geometry of which are both highly irregular. On the other hand are those with perfectly regular underlying topology — simple lattices and networks, equivalent packings and fused packings — but having irregular geometry. The latter are somewhat simpler to investigate and often much less expensive to work with. What has long been abundantly clear from all sides, however, is that even as limits, perfectly regular models and the concepts they support do not lead far toward understanding the nature of such porous media as reservoir rock.

CONCLUDING REMARKS

Regardless of the amount of irregularity in a reservoir rock, the connection patterns, or topologies, of the pore space and of the interpenetrating rock matrix are interrelated. To these also are related the distribution of curvature of the rock/pore surface, and the shapes of pores and grains. So too are the shape patterns, or geometries, of the pore space and rock matrix interrelated. These are the basic reasons that mechanical and transport properties of the solid matrix, fluid distribution properties of the pore space and flow and transport properties of the pore space are all interrelated. Structural character and transport processes depend on the connectivity structure, that is, the number and arrangement of transport paths, as well as on the material properties, cross-sectional areas, and shapes along those paths: topology is as important as geometry.

Together these basic considerations are points of departure for the goal of assembling a comprehensive picture of a rock on theoretical framework that is geologically sound, physically accurate, useful in defining and ranking needed experiments, and able to correlate measurements of all the important structural and transport properties.

ACKNOWLEDGEMENTS

The authors are grateful to James C. Hatfield for pioneering studies, Ronald G. Larson and Kishore K. Mohanty for their ongoing contributions, John P. Heller and James C. Melrose for their vision and encouragement the Mobil Education Foundation for crucial backing, and to the University of Minnesota Computer Center and the Fossil Energy Division of the U.S. Department of Energy for partial support of the research.

REFERENCES

1. Larson, R. G., Scriven, L. E., and Davis, H. T., "Percolation Theory of Residual Phases in Porous Media," Nature, 268, 409-413 (1977).

2. Larson, R. G., Davis, H. T., and Scriven, L. E., "Percolation Theory of Two-Phase Flow in Porous Media," Chem. Eng. Sci., to appear (1980).

3. Broadbent, S. R. and Hammersley, J. M., "Percolation Processes. I. Crystals and Mazes," Proc. Camb. Philos. Soc., 53, 629 (1956).

4. Kirpatrick, S., "Percolation and Conduction," Rev. Mod. Phys., 45 (4), 574-588 (1973).

5. Davis, H. T., Valencourt, L. R., and Johnson, C. E., "Transport Processes in Composite Media," 58, 446-452 (1975).

6. Ziman, J. M., *Models of Disorder*, Cambridge University Press, Cambridge, U.K. (1979).

7. Pathak, P., Ph.D. Thesis, University of Minnesota, in progress (1980).

8. Talmon, Y. and Prager, S., "Statistical Mechanics of Microemulsions," Nature, 267, 333-335 (1977).

9. Talmon, Y. and Prager, S., "Statistical Thermodynamics of Phase Equilibria in Microemulsions," J. Chem. Phys. 69, 2984-2991 (1978).

10. Hatfield, J. C., Ph.D. Thesis, University of Minnesota (1978).

11. Winterfeld, P. H., Ph.D. Thesis, University of Minnesota, in progress (1980).

12. Winterfeld, P. H., Scriven, L. E., and Davis, H. T., "An Application of Finite Element Analysis to Conductivity of Random Media," A.I.Ch.E. Preprint 31a, presented at the 87th National A.I.Ch.E. Meeting, Boston, MA, August, 1979.

13. Winterfeld, P. H., Scriven, L. E., and Davis, H. T., "A Percolation Model of Conduction in Random Media," J. Appl. Phys., to be submitted (1980).

14. Pathak, P., Scriven, L. E., and Davis, H. T., "Modelling the Mechanical Properties of Porous Media Using Voronoi Tesselations," J. Appl. Phys., to be submitted (1980).

15. Mohanty, K. K., Ph.D. Thesis, University of Minnesota, in progress (1980).

16. Ng, K. M., Davis, H. T., and Scriven, L. E., "Visualization of Blob Mechanics in Flow Through Porous Media," Chem. Eng. Sci., 33, 1009-1017 (1978).

17. Pesheck, P. S., Scriven, L. E., and Davis, H. T., "Cold Stage for Scanning Electron Microscopy of Volatile Systems," to be submitted, Rev. Sci. Instr. (1980).

18. Weinberg, L., *Network Analysis and Synthesis*, R. E. Kreiger, New York (1975).

19. Strang, G. and Fix, G., *An Analysis of the Finite Element Method*, Prentice-Hall Series in Automatic Computation, Englewood Cliffs, NJ (1973).

20. Kardestunger, H., *Elementary Matrix Analysis of Structures*, McGraw-Hill Book Company, New York (1974).

21. Rice, R. W., "Microstructure Dependence of Mechanical Behavior of Ceramics," *Treatise on Material Science and Technology, Vol. 11*, Ed. R. K. MacCrone, Academic Press (1977).

22. Brown, R. A., Orr, F. M., Jr., and Scriven, L. E., "Pore Character and Meniscus Movement in Diagenetically Altered Reservoir Rock," Can. J. Pet. Tech., to appear (1980).

23. Scriven, L. E., "Equilibrium Bicontinuous Structures," *Micellization, Solubilization and Microemulsions, Vol. 2*, Ed. K. L. Mittal, Plenum Press (1977) pp. 877-895.

24. Mohanty, K. K., Davis, H. T., and Scriven, L. E., "Thin-Films and Fluid Distributions in Porous Media," presented at the 3rd International Conference on Surface and Colloid Science, Stockholm, Sweden, August 20-25, 1979.

25. Mohanty, K. K., Davis, H. T., and Scriven, L. E., "Stability of Thin Fluid Films at Rest on Simply Shaped Solids," A.I.Ch.E. Preprint No. 121a, presented at the A.I.Ch.E Annual Meeting, San Francisco, CA, November, 1979.

26. Larson, R. G., Davis, H. T., and Scriven, L. E., "Displacement of Residual Nonwetting Fluid From Porous Media," Chem. Eng. Sci., to appear (1980).

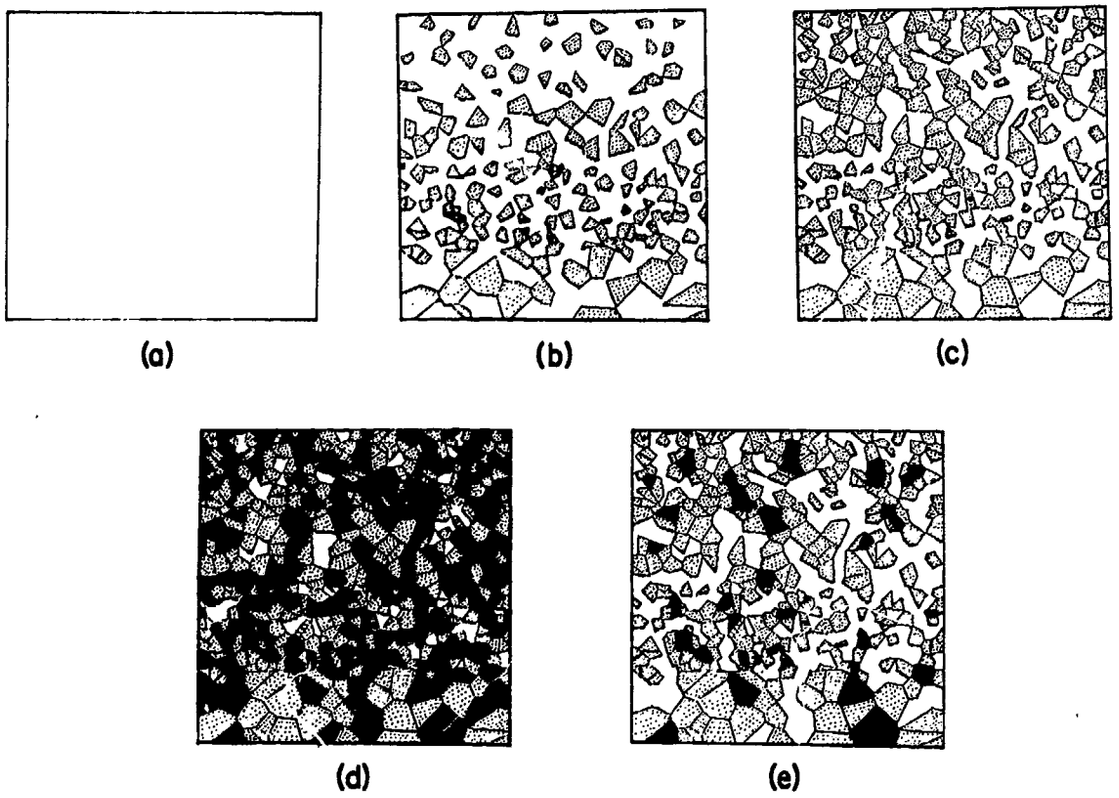

Fig. 1 - Rock history. Stippled areas -- grains; open -- brine; black -- oil.

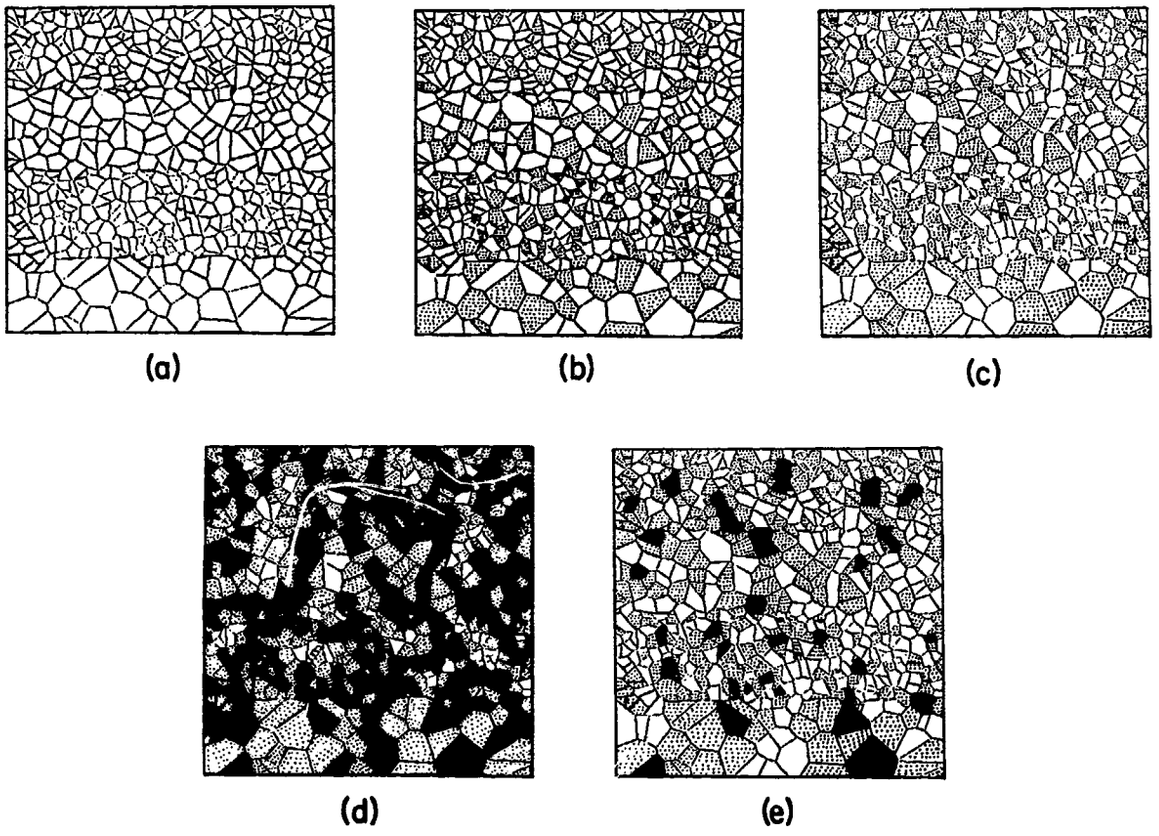

Fig. 2 - Polygon assemblages representing the stages in Fig. 1.

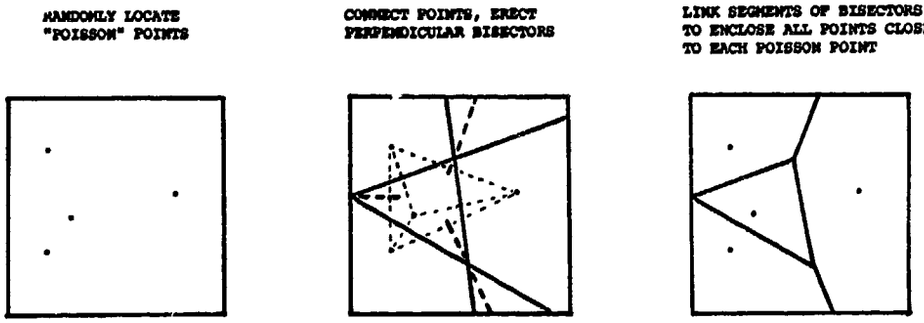

Fig. 3 - Construction of a Voroni tesselation.

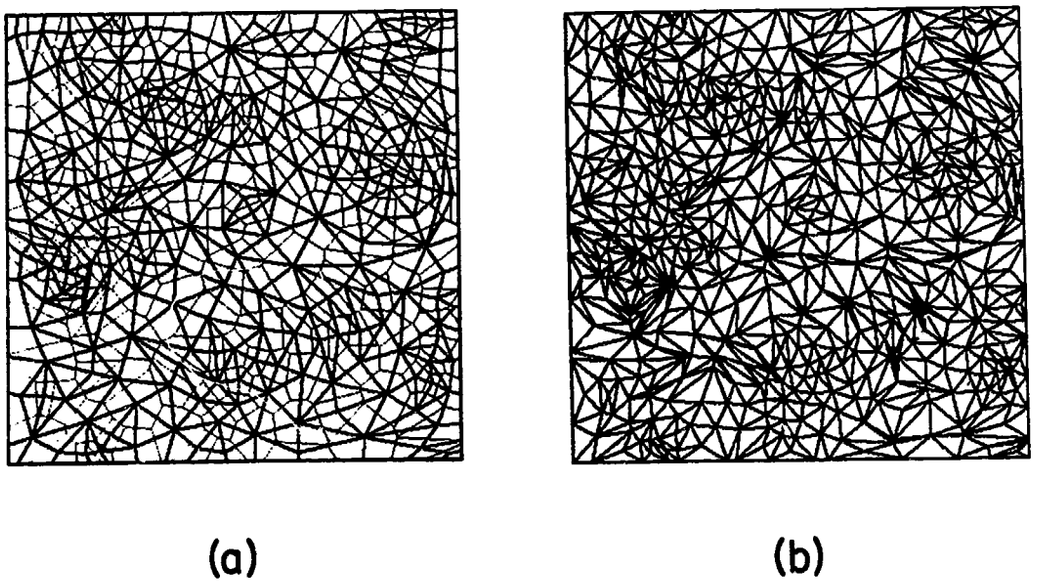

Fig. 4 - Network, (a), and triangulation, (b), of a tesselation.

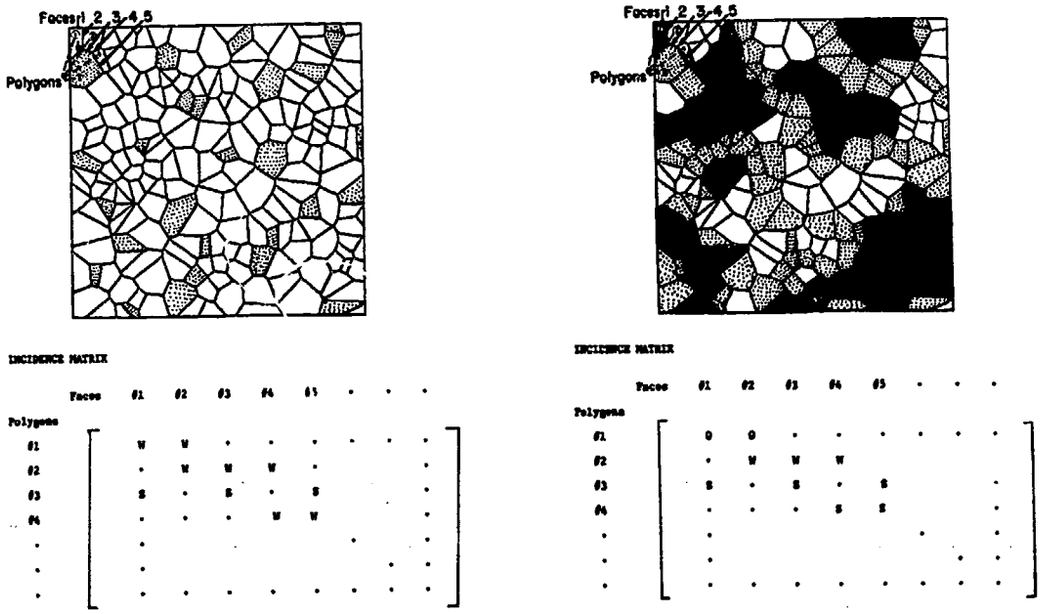

Fig. 5 - Incidence matrices representing structure. S -- solid; W -- brine; O -- oil. (Polygons and edges are separately numbered.)

OHM'S LAW	$J = -K\frac{\Delta\phi}{\Delta L}$	SCALAR AND LINEAR
FOURIER'S LAW	$Q = -K\frac{\Delta T}{\Delta L}$	SCALAR AND LINEAR
DARCY'S LAW	$V = -\frac{k}{\mu}\frac{\Delta p}{\Delta L}$	SCALAR AND LINEAR
HOOKE'S LAW IN ONE DIMENSION OR IN "LOCAL COORDINATES"	$\frac{F}{A} = E\frac{\Delta L}{L}$	SCALAR AND LINEAR
HOOKE'S LAW IN GENERAL	$\frac{\underline{F}}{A} = E\underline{\underline{R}}(\underline{x}) \cdot \frac{\Delta \underline{x}}{L}$	VECTOR AND NONLINEAR ($\underline{\underline{R}}$ IS A ROTATOR)
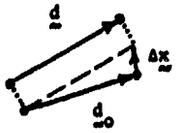	$\frac{E}{A} = E\frac{\underline{d}}{\lvert\underline{d}\rvert}\left(\frac{\lvert\underline{d}\rvert - \lvert\underline{d}_o\rvert}{\lvert\underline{d}_o\rvert}\right)$	ALTERNATIVE FORM

Fig. 6 - Constitutive relations between flux and potential.

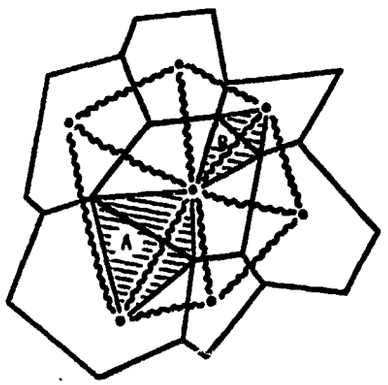

A NETWORK OF 7 SITES (DOTS) AND 12 BONDS (WAVY LINES) SUPERIMPOSED OVER THE CORRESPONDING 7 VORONOI POLYGONS. THE SHADED AREAS, A AND B, REPRESENT ONE WAY TO SUBDIVIDE THE TESSELATION SO THAT ITS CONDUCTIVE BEHAVIOR IS MODELED BY THE CORRESPONDING BOND NETWORK.

Fig. 7 - Network transport property from Voronoi tesselation.

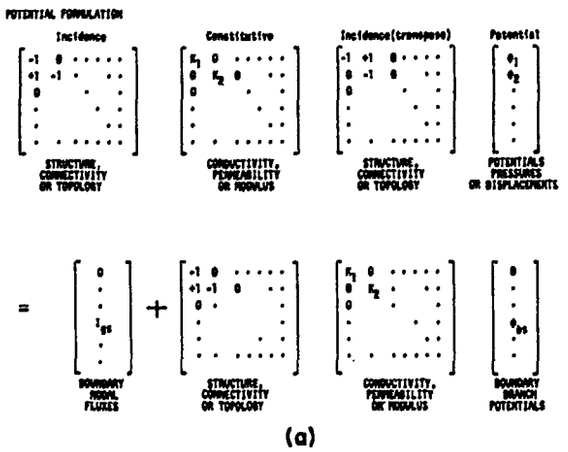

(a)

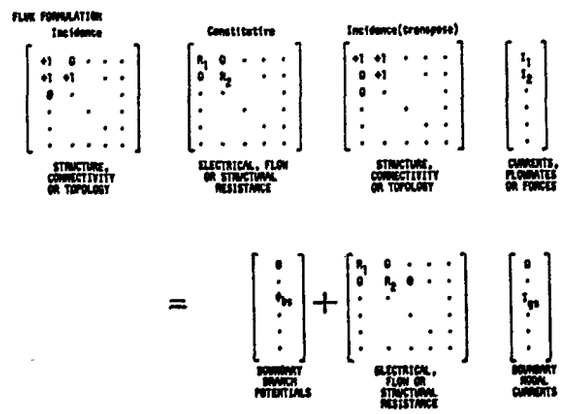

(b)

Fig. 8 - Matrix representation of transport problems.

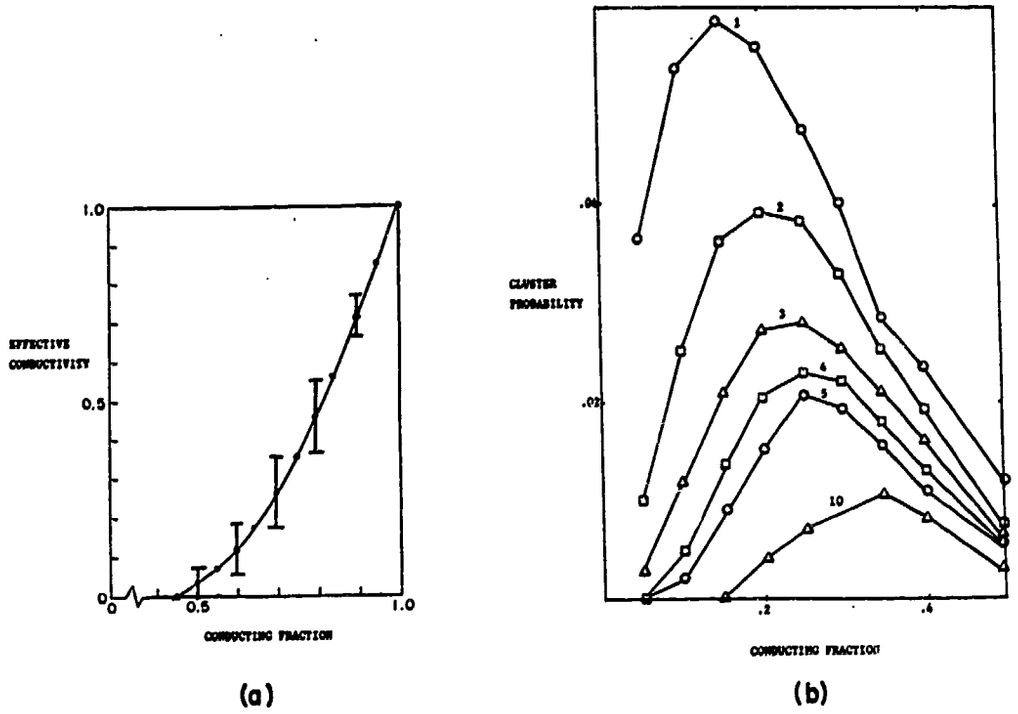

Fig. 9 - Conductivity of network model, (a), and size distribution of conducting clusters, (b), vs. fraction of conducting branches.

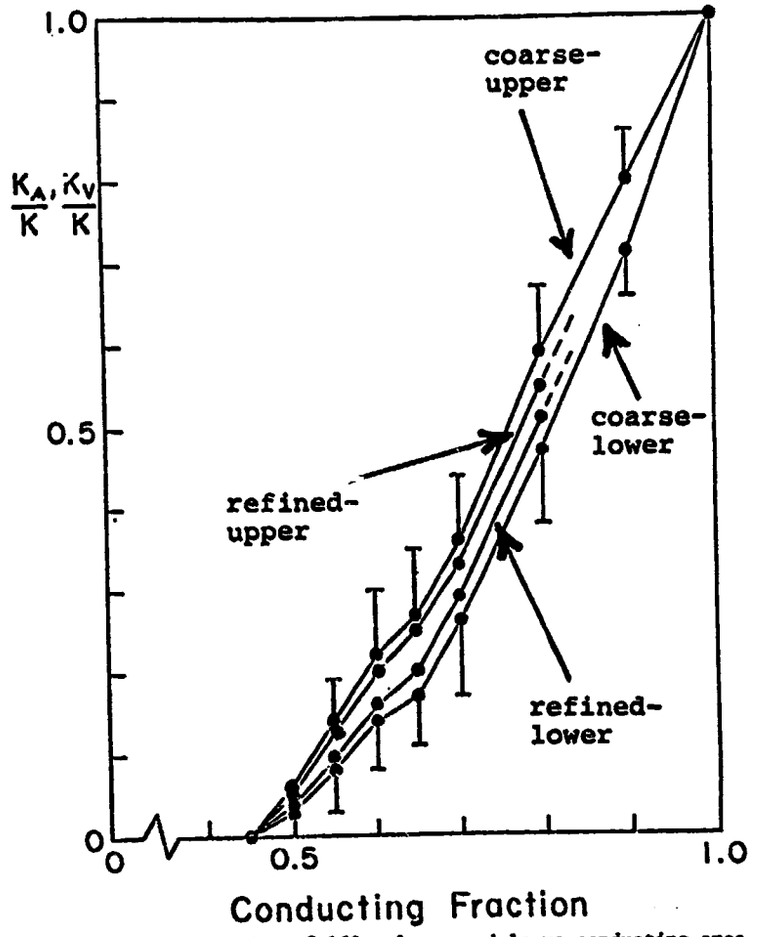

Fig. 10 - Conductivity of 160-polygon models vs conducting area fraction, calculated by finite element method. V-potential formulation, A-flux formulation.

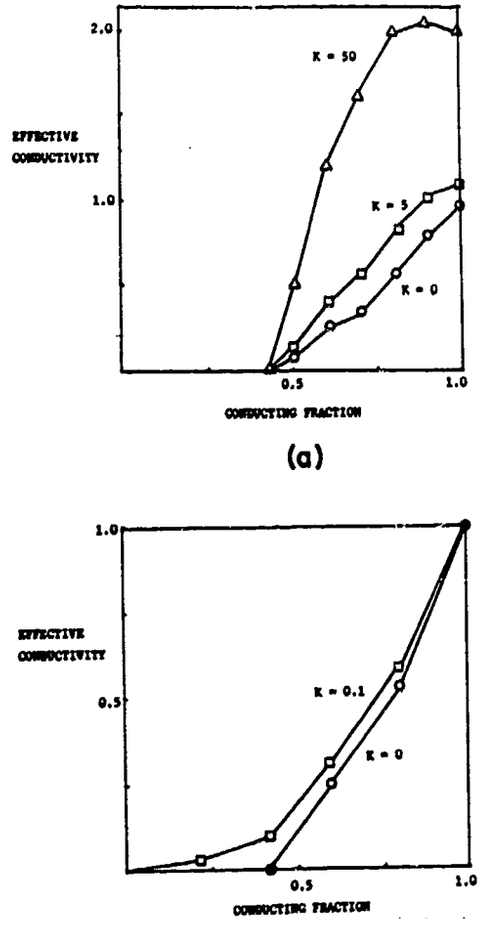

Fig. 11 - Effects of pore surface conduction, (a), and, additionally, grain boundary conduction, (b), by finite element method.

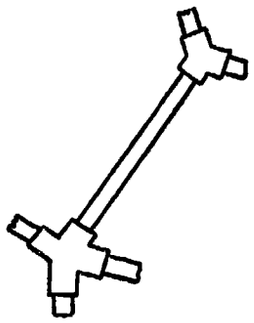

RIGID-JOINTED STRUCTURE

$$\begin{bmatrix} F_x \\ F_y \\ M_z \end{bmatrix} = \begin{bmatrix} \frac{EA}{L}\cos^2\theta + \frac{12EI}{L^3}\sin^2\theta & (\frac{EA}{L} - \frac{12EI}{L^3})\cdot\cos\theta\sin\theta & \frac{6EI}{L^2}\sin\theta \\ & \frac{EA}{L}\sin^2\theta + \frac{12EI}{L^3}\cos^2\theta & -\frac{6EI}{L^2}\cos\theta \\ \text{Symmetric} & & \frac{4EI}{L} \end{bmatrix} \begin{bmatrix} \Delta x \\ \Delta y \\ \Delta\phi \end{bmatrix}$$

Fig. 12 - Rigid-jointed truss element and stress-strain relation at each point.

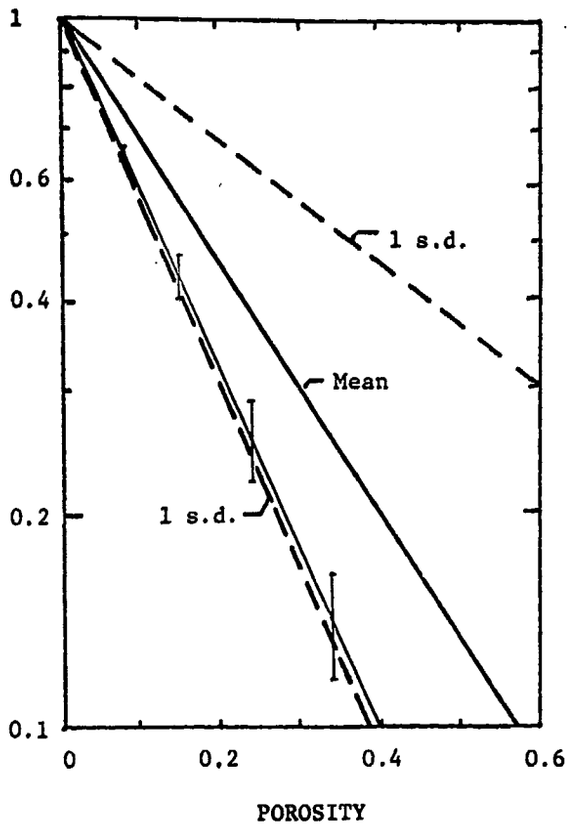

Fig. 13 - Young's modulus vs porosity, calculated from two-dimensional network model. Experimental data band from Rice.[21]

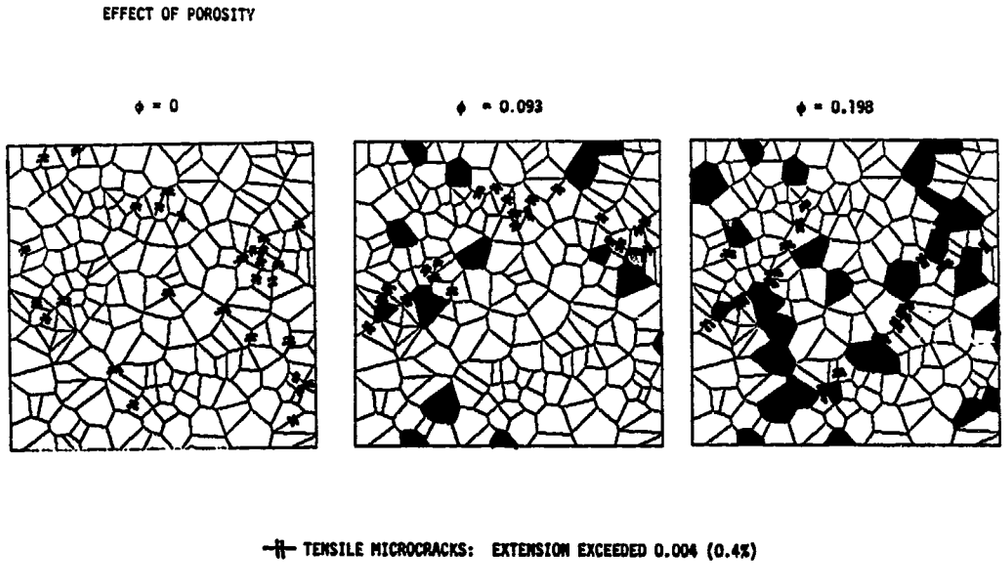

Fig. 14 - Microcracking at maximum stress, calculated from two-dimensional truss network models of different porosities.

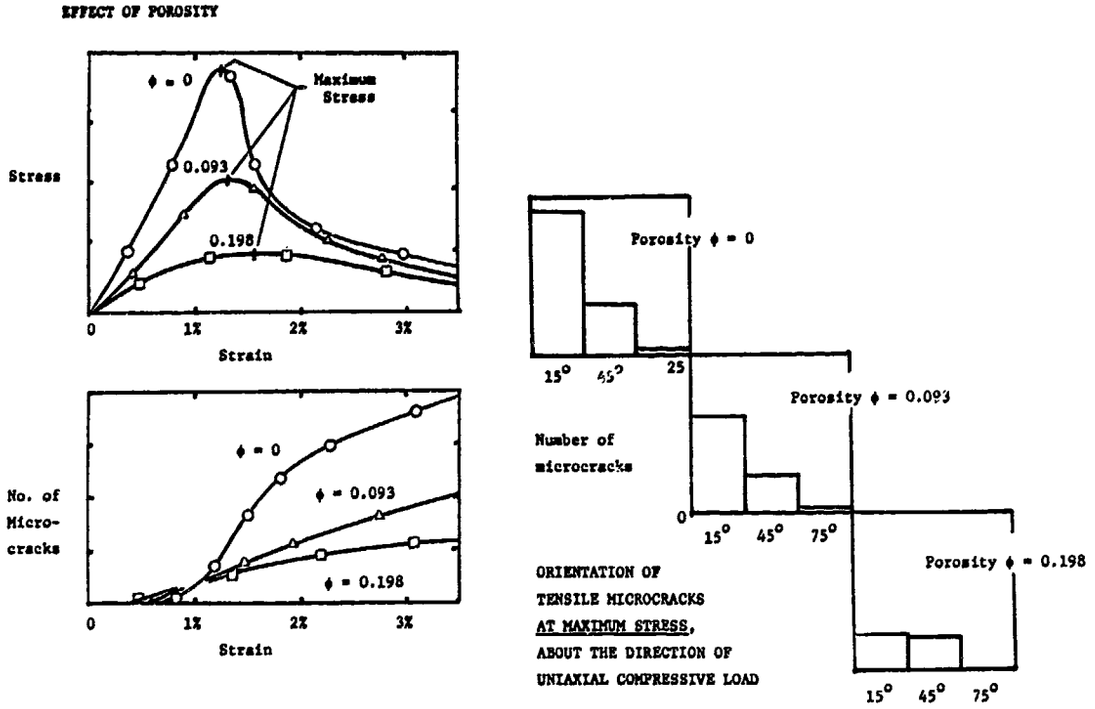

Fig. 15 - Stress, strain, and orientation of microcracking in two-dimensional truss network models.

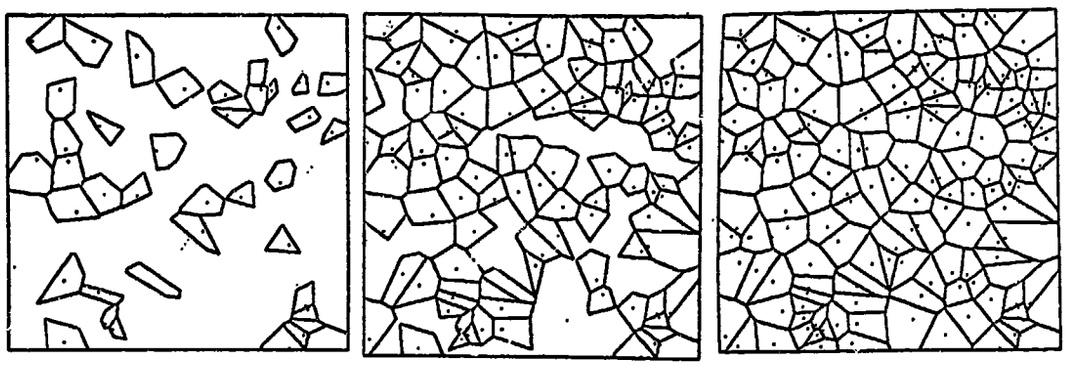

Fig. 16 - A continuous path appears as conducting elements are added randomly: the percolation threshold.